MOLECULAR AND CELLULAR BIOLOGY, June 1993, p. 3494–3504
0270-7306/93/063494-11$02.00/0

Vol. 13, No. 6

Hel-N1: an Autoimmune RNA-Binding Protein with Specificity for 3′ Uridylate-Rich Untranslated Regions of Growth Factor mRNAs

TODD D. LEVINE, FENBIAO GAO, PETER H. KING,† LUCY G. ANDREWS, AND JACK D. KEENE*

Department of Microbiology and Immunology, Duke University Medical Center, Durham, North Carolina 27710

Received 30 December 1992/Returned for modification 18 February 1993/Accepted 26 March 1993

We have investigated the RNA binding specificity of Hel-N1, a human neuron-specific RNA-binding protein, which contains three RNA recognition motifs. Hel-N1 is a human homolog of *Drosophila melanogaster elav*, which plays a vital role in the development of neurons. A random RNA selection procedure revealed that Hel-N1 prefers to bind RNAs containing short stretches of uridylates similar to those found in the 3′ untranslated regions (3′ UTRs) of oncoprotein and cytokine mRNAs such as c-*myc*, c-*fos*, and granulocyte macrophage colony-stimulating factor. Direct binding studies demonstrated that Hel-N1 bound and formed multimers with c-*myc* 3′ UTR mRNA and required, as a minimum, a specific 29-nucleotide stretch containing AUUUG, AUUUA, and GUUUUU. Deletion analysis demonstrated that a fragment of Hel-N1 containing 87 amino acids, encompassing the third RNA recognition motif, forms an RNA binding domain for the c-*myc* 3′ UTR. In addition, Hel-N1 was shown to be reactive with autoantibodies from patients with paraneoplastic encephalomyelitis both before and after binding to c-*myc* mRNA.

RNA-binding proteins are involved in a variety of regulatory and developmental processes such as RNA processing and compartmentalization, mRNA translation, and viral gene expression. One family of RNA-binding proteins is defined by the presence of an 80-amino-acid RNA recognition motif (RRM) which was shown to constitute the core structure of the RNA binding domain of the U1snRNP-70K protein (39). The motif characteristic of this family of proteins is evident from the conservation of several amino acid residues, most notably RNP1 and RNP2 consensus sequences (1, 4, 26, 27). On the basis of crystallographic and nuclear magnetic resonance spectroscopic studies of the U1 RNA binding domain of the U1snRNP-A protein, a model of the RRM tertiary structure has been derived (21, 36). The structural model of the domain together with biochemical studies has led to the suggestion that the RNA binding surface resides within a monomeric unit domain containing four antiparallel β strands with solvent-exposed aromatic and basic residues (27).

More than 100 members of the RRM superfamily have been reported, the majority of which are expressed in all tissues and are conserved throughout phylogeny (27). Tissue-specific members of the RRM superfamily are less common but include X16, which is expressed in pre-B cells (3); Bj6, which is a puff-specific *Drosophila melanogaster* protein (62); and *elav* (embryonic lethal abnormal vision), which is a neuron-specific protein in *D. melanogaster* (44). The natural RNA ligands have been identified for a few RRM-containing proteins; however, RNA ligands have not been reported for these tissue-specific RRM proteins. In order to understand the functions of tissue-specific RRM proteins in cellular RNA metabolism, it is essential to identify RNAs with which they interact.

In this study, we characterized the in vitro RNA binding specificity of a human neuron-specific counterpart to *elav* called Hel-N1 (human *elav*-like neuronal protein 1). *elav* contains three RRMs and has been shown to be vital for the proper migration and differentiation of the *D. melanogaster* nervous system (43, 44). However, to date no known RNA ligands for *elav* have been elucidated. Selection of RNAs from degenerate pools of in vitro transcripts demonstrated that Hel-N1 preferred to bind RNAs which resemble sequences in the 3′ untranslated regions (UTRs) of certain mRNAs. Direct binding studies revealed that Hel-N1 can bind specific portions of the 3′ UTR of rapidly degraded mRNAs, such as c-*myc*, c-*fos*, and granulocyte macrophage colony-stimulating factor (GM-CSF). Interestingly, despite the neuron-specific localization of *elav*-like proteins (43) and the ability of Hel-N1 to bind growth factor mRNAs, N-*myc* mRNA was not capable of binding. Furthermore, the carboxy-terminal RRM (RRM3), comprising 87 amino acids of Hel-N1, was shown to be sufficient for binding to the c-*myc* 3′ UTR. These findings are discussed with respect to the genetic lesions in *elav* and the autoimmune properties of *elav*-like mammalian proteins.

MATERIALS AND METHODS

Expression of Hel-N1 constructs in *Escherichia coli*. Recombinant Hel-N1 was expressed in the T7 RNA polymerase expression system (45) as a fusion protein with a 13-amino-acid peptide tag termed g10 (58). A diagram depicting *elav*, Hel-N1, and deletion constructs of Hel-N1 is shown in Fig. 1. The Hel-N1/RRM1 construct contained amino acid residues 1 to 161 including all of RRM1 and 35 residues of RRM2, and Hel-N1/RRM1,2′ contained amino acid residues 1 to 186, which include all of RRM1 and 60 residues of RRM2. The Hel-N1/RRM3 construct contained the carboxy-terminal 87 amino acid residues 272 to 358. The entire Hel-N1 sequences and sites comprising the deletion constructs will be published elsewhere (29a). After transformation of each construct into *E. coli* BL21(DE3)pLysS (45), the

* Corresponding author.
† Present address: Department of Neurology, University of Alabama Medical Center, Birmingham, AL 35294.

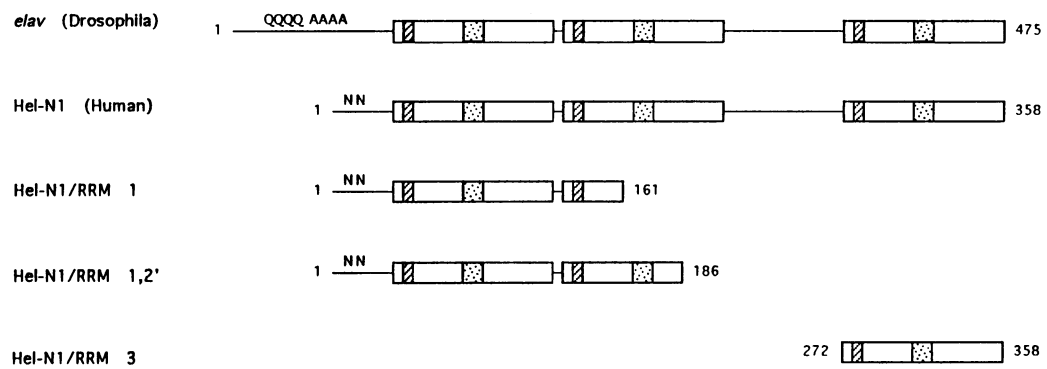

FIG. 1. Diagram comparing the basic structure of human Hel-N1 with that of the *D. melanogaster elav* protein. Three subconstructs of Hel-N1 are shown also. Open boxes represent the RRMs, and shaded regions represent RNP1 and RNP2 (reviewed in reference 27). The amino acid residues contained within each construct are indicated on the right and left ends of the structures.

bacteria were grown in Luria-Bertani broth at 37°C to an optical density at 500 nm of 0.3 and induced with 1.0 mM IPTG (isopropyl-β-D-thiogalactopyranoside) as described earlier (38). Cells were harvested by centrifugation, washed twice, and resuspended in 10 ml of *E. coli* lysis buffer (50 mM Tris-HCl [pH 7.5], 100 mM NaCl, 10 mM EDTA, 0.05% Nonidet P-40, 1 mM dithiothreitol [DTT], and 0.25 mM phenylmethylsulfonyl fluoride). Lysis was completed by freeze-thawing of the cells, followed by 60 s of sonication. The extract was centrifuged at 10,000 × *g* for 30 min to remove insoluble debris. Hel-N1 was partially purified by removing the nucleic acids with 1% polyetheneimine and fractionated on S-Sepharose (Pharmacia) with a linear gradient of NaCl at pH 8.2. Fractions containing Hel-N1 contained no other proteins distinguishable by Coomassie blue staining of 10% polyacrylamide gel electrophoresis (PAGE) gels.

RNA selection procedure. RNA selection was according to the method described by Tsai et al. (56). Briefly, an oligodeoxynucleotide containing a T7 promoter sequence (T7 Univ) at the 5′ end, followed by 25 degenerate nucleotides and then a reverse universal primer sequence (Rev Univ) at the 3′ end, was used in a 35-cycle polymerase chain reaction (PCR) under the following conditions: 1 min at 94°C, 1 min at 50°C, and 2 min at 72°C, all in 10 mM Tris-HCl (pH 8.3), and 50 mM KCl–1.5 mM $MgCl_2$–0.01% gelatin–0.1 μg each of T7 Univ and Rev Univ primers–200 mM deoxynucleoside triphosphates–2.5 U of *Taq* DNA polymerase. With the PCR products as a template for transcription, RNA was synthesized with the T7 polymerase transcription system (48). The degenerate pool of synthetic RNA was incubated with g10–Hel-N1 fusion protein which had been prebound to a rabbit antibody directed against the g10 peptide tag and protein A beads (Sigma). The pelleted beads were subsequently washed five times with NT2 buffer (50 mM Tris-HCl [pH 7.5], 150 mM NaCl, 1 mM $MgCl_2$, 0.05% Nonidet P-40), and the immunoprecipitated RNA was phenol extracted and ethanol precipitated in the presence of 10 μg of carrier yeast tRNA (Sigma). The RNA was resuspended in 10 μl of water, and 3 μl was used for PCR amplification under conditions described above. The T7 and Rev Univ primers had *Bam*HI restriction sites incorporated at the 5′ ends such that any resultant concatamers were reduced to monomers upon *Bam*HI digestion. This process was repeated two additional times before the products were subcloned into pGEM-3Zf(+) and sequenced.

Plasmids and mRNA transcripts. Constructs containing the 3′ UTRs of the human GM-CSF gene, the c-*fos* gene, and the c-*myc* gene were graciously provided by E. Vakalopoulou (60) and are shown in Fig. 2. The plasmids were linearized as follows: GM-CSF RNA was digested with *Bgl*II and transcribed with SP6 RNA polymerase, generating a 266-nucleotide (nt) RNA transcript; pGEM3 plasmid containing c-*fos* DNA was linearized with *Nae*I and transcribed with T7 RNA polymerase to yield a 620-nt RNA; and pGEM3 plasmid containing c-*myc* DNA was linearized with *Bam*HI and transcribed with SP6 RNA polymerase, yielding a 432-nt transcript. For binding of truncated transcripts of the c-*myc* 3′ UTR to Hel-N1, ^{32}P-labeled SP6 transcripts were synthesized from the above pGEM3/*myc* construct linearized with the following restriction enzymes: *Bam*HI (432-nt RNA, full-length transcript), *Rsa*I (293-nt transcript), *Ssp*I (219-nt transcript), *Dra*I (181-nt transcript), and *Mse*I (152-nt transcript) as depicted by the arrows in Fig. 2.

RNA binding to Hel-N1. For each binding reaction, 4 mg of protein A beads was washed three times in NT2 buffer. Five microliters of rabbit anti-g10 antibody, or 20 μl of human serum from patients with paraneoplastic encephalomyelitis (PEM), was incubated with protein A for 10 min on ice and washed three times with NT2 buffer. Recombinant Hel-N1 contained in 35 μl of extract was added, incubated 10 min on ice, and washed three times with NT2 buffer. After the final wash, the antibody-protein complex was resuspended in 0.1 ml of RNA binding buffer [20 mM KCl, 150 mM NaCl, 50 mM Tris-HCl (pH 7.5), 0.05% Nonidet P-40, 2.5% polyvinyl alcohol, 1 mM $MgCl_2$, 1 mM ethylene glycol-bis(β-aminoethyl ether)-*N,N,N′,N′*-tetraacetic acid (EGTA), 0.5 mg of *Saccharomyces cerevisiae* tRNA per ml, 0.05 mg of poly(A) per ml, 1 mM DTT, 0.125 mg of bovine serum albumin (BSA) per ml, 0.4 mM vanadyl ribonucleoside complex, 80 U of RNasin per ml], and equimolar amounts of labeled transcripts were added. After 5 min of incubation at room temperature, the binding reaction mixture was washed five times with NT2, 0.1 ml of water–13 μl of 5 M NaCl–1 μl of 10 mg of yeast tRNA per ml was added, and the mixture was PCl extracted and ethanol precipitated. The pelleted RNA was analyzed by 6% urea–PAGE. Supernatants from the binding reaction mixtures were analyzed also to confirm that intact transcripts were available for binding by Hel-N1.

Transfection of COS cells. COS cells were grown in Iscove's medium supplemented with 10% fetal calf serum and penicillin and streptomycin to 70% confluence. A transfection cocktail containing 50 μl of phosphate-buffered saline (PBS), 0.125 μg of DNA for each vector, and 1.25 μl of a

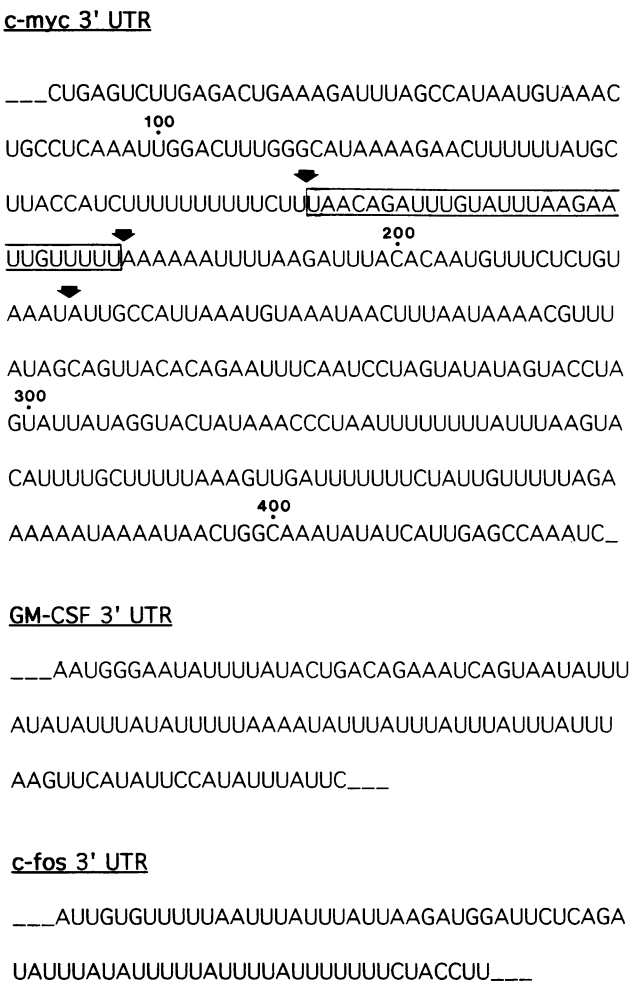

FIG. 2. RNA sequences in the 3′ UTRs of c-*myc*, GM-CSF, and c-*fos* mRNAs as depicted by Vakalopoulou et al. (60) which share the highest degree of homology. Arrows indicate the truncation sites for producing the in vitro RNA transcripts of c-*myc* 3′ UTR used in the experiment shown in Fig. 5. The boxed region indicates a sequence required for Hel-N1 binding.

10-mg/ml solution of DEAE-dextran was prepared. This cocktail was added directly to cells washed with PBS and incubated for 30 min at 37°C. A total of 500 μl of medium was added to the dish with chloroquine at a final concentration of 100 μM. After incubation for 2.5 h at 37°C, the cells were washed with PBS and 500 μl of medium containing 10% dimethyl sulfoxide was added for 2.5 min and then replaced with fresh medium. After 48 h, the cells were washed twice in PBS and pelleted. Following resuspension in 1 ml of SM buffer (100 mM NaCl, 50 mM Tris-HCl [pH 7.4], 1 mM DTT, 2 U of RNasin, 2 μl of vanadyl ribonucleoside complex), the cells were sonicated and centrifuged at 3,000 × *g* for 5 min at 4°C.

RNase protection. The supernatant from COS cell extracts was added to 5 mg of protein A which was prebound to 5 μl of g10 rabbit serum. The bound RNA was ethanol precipitated, dried, and resuspended in 30 μl of hybridization buffer [800 μl of formamide, 40 μl of 1 M piperazine-*N*,*N*′-bis(2-ethanesulfonic acid) (PIPES) (pH 6.4), 80 μl of 5 M NaCl, 2 μl of 0.5 M EDTA, 78 μl of diethylpyrocarbonate water). The solution was then heated for 10 min at 85°C and allowed to hybridize overnight at 45°C. A total of 300 μl of RNase buffer was added (915 μl of water, 30 μl of 1 M Tris [pH 7.5], 30 μl of 0.5 M EDTA, 180 μl of 5 M NaCl) together with 18 μl of RNase A (10 mg/ml)–3 μl of RNase T_1 (Sigma) and incubated for 1 h at 30°C. Digestion was stopped with 20 μl of 10% sodium dodecyl sulfate (SDS) and 2.5 μl of proteinase K with incubation for 15 min at 37°C. A total of 15 μg of carrier tRNA was added, and the solution was PCl extracted twice. RNA was ethanol precipitated, dried, and analyzed by 6% PAGE. The probe for RNase protection assays corresponded to the first 46 nt of the 3′ UTR of c-*myc* in the pGEM3 construct.

UV cross-linking. HeLa cell nuclear extracts were prepared as described by Dignam et al. (17). A total of 500,000 cpm of ^{32}P-labeled transcripts and 5 μg of nuclear extract were combined in a microtiter plate, and label transfer from RNA to protein was carried out as described by Wilusz et al. (63). RNase A was added to a final concentration of 1 mg/ml, and the solution was incubated for 15 min at 37°C. Label transfer to Hel-N1 was carried out similarly, except that the protein was dissolved in a UV cross-linking buffer (20 mM HEPES [*N*-2-hydroxyethylpiperazine-*N*′-2-ethanesulfonic acid], 1 mM $MgCl_2$, 60 mM KCl, 10% glycerol). Competition experiments included 5 μg of HeLa cell nuclear extract in the presence of increasing amounts of Hel-N1, maintaining a total reaction volume of 10 μl. Cross-linked complexes were solubilized in Laemmli buffer and analyzed on an SDS–10% polyacrylamide gel.

Mobility shift analysis. Analysis of RNA-protein complexes using nondenaturing acrylamide gels was as described previously (6, 26, 36). [^{32}P]UTP-labeled c-*myc* or GM-CSF 3′ UTR RNAs were incubated with partially purified Hel-N1 in 50 μl of RNA binding buffer and incubated at room temperature for 10 min. RNA-protein complexes were resolved by electrophoresis through a 3.2% nondenaturing polyacrylamide gel with 0.5× TBE (final concentrations of 45 mM Tris-boric acid and 1 mM EDTA) as the running buffer. Gels were preelectrophoresed at 4°C for 1 h at 12 V/cm prior to loading the reaction mixture, and electrophoresis proceeded for an additional 3 to 4 h at a constant voltage.

RESULTS

Hel-N1 selects uridine-rich sequences for RNA binding. Hel-N1 was cloned from a fetal brain cDNA library with degenerate oligonucleotides and PCR and found to possess three RRMs as represented in Fig. 1. The cloning, sequence analysis, and neuronal localization of Hel-N1 will be presented elsewhere (29a). The putative RNA binding domains of Hel-N1 are highly homologous to two neuronal proteins from *D. melanogaster*, *elav* and K3(*rbp9*). However, the RNA binding specificities of *elav*, K3, and Hel-N1 are not known. Thus, several standard RNA binding assays were employed to identify an RNA structure capable of binding Hel-N1. For example, radiolabeled whole-cell RNA from HeLa cells, neuroblastomas, and glioblastomas was used for binding to Hel-N1 but did not reveal a cognate RNA species (data not shown). As an alternative approach, we used a random RNA selection procedure described previously (56) to identify RNA sequences preferred for binding to Hel-N1.

The RNA selection procedure utilized a synthetic DNA of 80 nt which contained a stretch of 25 degenerate nucleotides in the center and is similar to methods used by other investigators to identify preferred RNA-binding ligands (5, 19, 56–59). The sequences flanking the degenerate sequence

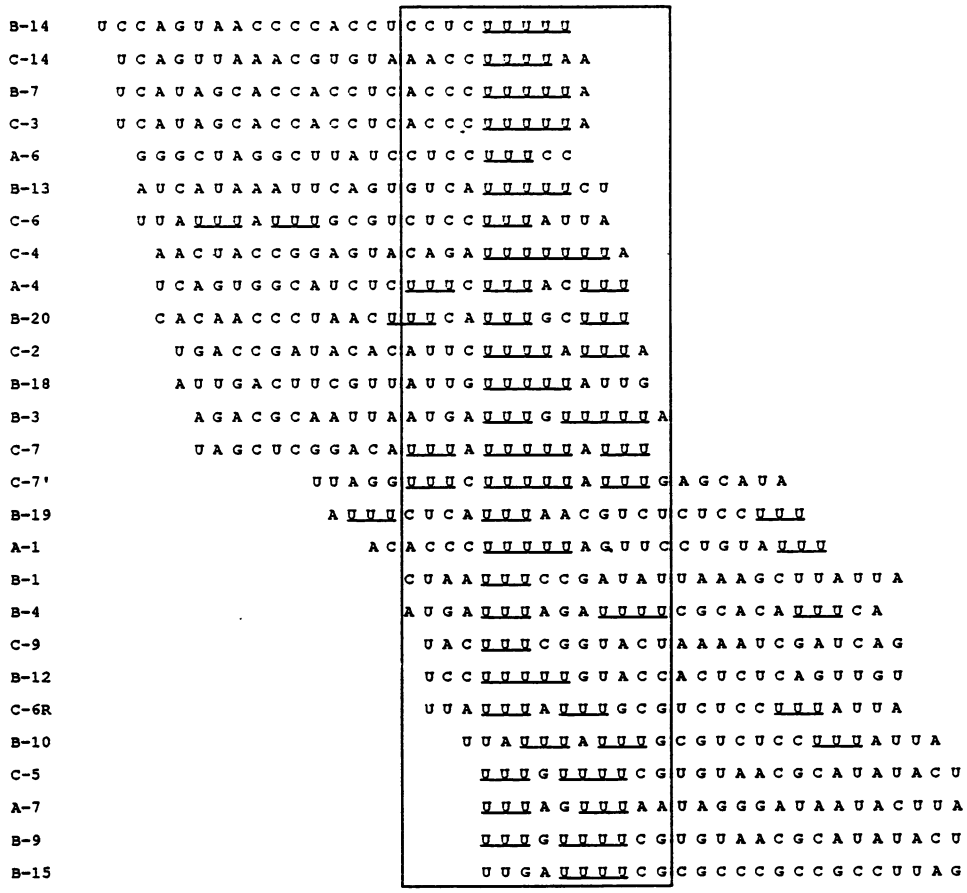

FIG. 3. RNA sequences selected to bind Hel-N1 by a random RNA selection procedure. Twenty-eight RNAs, each 25 nt in length, were identified from clones generated by reverse transcription and PCR amplification. Twenty-six of the sequences contained short stretches of uridylate residues interspersed with other nucleotides. Note that C-6 and C-6R are the same sequence. The boxed region highlights the most conserved uridylate-rich regions that appeared among the selected RNAs.

included a T7 promoter for synthesis of RNA and flanking PCR primer sites to regenerate the template. In vitro transcripts from this template constituted a large heterogeneous pool of RNAs which represent potential binding sequences (56). After binding of recombinant Hel-N1 to the degenerate RNA pool and immunoprecipitation of the complex by using the g10 epitope tag (6, 58), bound RNAs were eluted. By standard reverse transcription and PCR, DNA templates encoding the bound RNAs were amplified and used again for RNA synthesis. After two additional cycles of binding and selection, 28 independent cDNA clones representing individual RNA species were evaluated by sequence analysis. The striking finding was the preponderance of uridylate residues in short stretches interrupted by other nucleotides (Fig. 3). These U-rich stretches were characteristically 3 to 5 nt in length and were similar to sequences found in the 3′ UTRs of oncoprotein and lymphokine mRNAs (Table 1) which have been postulated to confer short half-lives on these messages (12, 51). Interestingly, among the short U-rich sequences selected, most could be found in one or more of the 3′ UTRs of the oncoprotein and lymphokine mRNAs (51). It is known that the sequences present in these 3′ UTRs tend to be AU-rich; however, publications to date have failed to arrive at a consensus motif responsible for the instability observed among the wide variety of mRNAs with short half-lives. Several investigators have noted the frequent occurrence of the pentamer AUUUA.

When used previously in our laboratory with other members of the RRM family of proteins, the random RNA selection procedure did not yield RNAs containing U-rich sequences (references 56–58 and unpublished data). Thus,

TABLE 1. RNA sequences containing short stretches of uridylates, selected from random RNA libraries by binding to Hel-N1[a]

Uridylate stretch	Instability region(s)[b]
AUUUA	GM-CSF, IFN-α, IFN-β, IFN-γ, IL-1, IL-2, IL-3, c-*myc*, c-*myb*
UAUUUAU	TNF, IFN-α, GM-CSF, IL-2, c-*fos*
AUUUUUA	GM-CSF, IFN-β, c-*myb*, c-*fos*, IgG1-IF, IL-2
AUUUUA	GM-CSF, IFN-β, c-*myc*, IL-2, c-*fos*, c-*myb*
GUUUUUA	c-*myc*, c-*fos*
CUUUUUA	IFN-β, c-*myc*
AUUUG	c-*myb*, c-*myc*
AUUUC	c-*sis*, c-*myc*
CUUUUA	c-*sis*, IL-2
AUUUUC	IFN-β
CUUUA	IL-2, c-*myc*

[a] The selected sequences listed were derived from those shown in Fig. 3 and in other experiments and are present in the 3′ UTRs of mRNAs described by Shaw and Kamen (51) as representing instability regions.

[b] IFN-α, -β, and -γ, alpha, beta, and gamma interferons, respectively; IL-1, -2, and -3, interleukin-1, -2, and -3; TNF, tumor necrosis factor; IgG1-IF, immunoglobulin G1-induction factor.

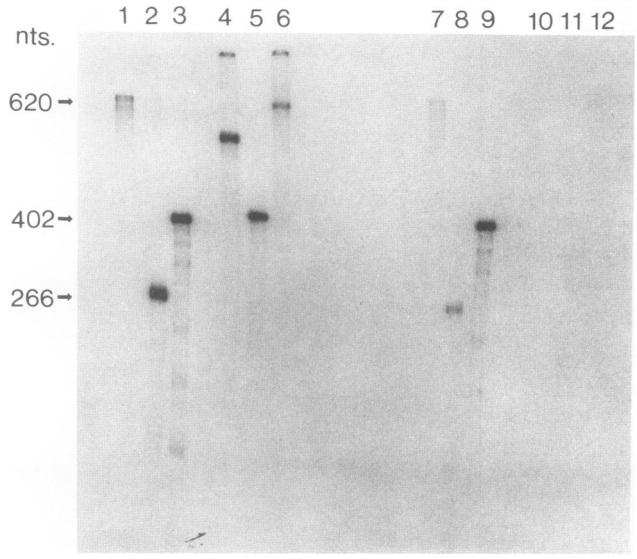

FIG. 4. Binding of growth factor RNAs to g10-tagged Hel-N1 protein with immunoprecipitation with g10 antibody. Lanes: 1 to 6, transcripts remaining in the supernatants after the first step of binding; 7 to 12, RNAs extracted from the Staph A pellets after five washes; 1 and 7, 3′ UTR of c-*fos* mRNA; 2 and 8, 3′ UTR of GM-CSF mRNA; 3 and 9, 3′ UTR of c-*myc* mRNA; 4 and 10, 580-nt transcript of U1snRNP-70K mRNA; 5 and 11, 426-nt antisense transcript of hY1 gene; 6 and 12, 632-nt transcript of 3′ UTR of N-*myc* mRNA. The 3′ UTR sequences of c-*myc*, c-*fos*, and GM-CSF were derived from the constructs of Vakalopoulou et al. (60) and as described in Materials and Methods. Approximately equimolar quantities of each radiolabeled transcript were added together with tRNA and poly(A) competitors to g10 epitope-tagged Hel-N1 protein which was prebound to Staph A-Sepharose beads via g10-specific antiserum. RNAs were analyzed on a urea–8% acrylamide gel.

the U-rich sequence derived with recombinant Hel-N1 was unique and highly reproducible in that only 2 of the 28 sequences did not contain the U-rich pattern (data not shown). These variants were rare in the population and thus may represent ligands of lower binding affinity. Alternatively, because Hel-N1 contains three potential RNA binding domains, these other sequences may represent ligands which were bound by one of the domains not involved in recognition of the U-rich regions. This possibility is compatible with the proposal that Hel-N1 may exist as a ribonucleoprotein (RNP) by interacting with two or more RNAs via its multiple RRMs (33).

Hel-N1 binds to transcripts containing the 3′ UTR of c-*myc*, c-*fos*, and GM-CSF mRNA. To address the question of whether recombinant Hel-N1 could bind the 3′ UTRs of oncoprotein and lymphokine mRNAs, DNA constructs encoding sequences of the 3′ UTR of c-*myc*, c-*fos*, and GM-CSF mRNAs (Fig. 2) were used to synthesize radiolabeled transcripts for binding studies (6, 48, 60). Hel-N1 was expressed in *E. coli* as a fusion construct containing a 13-amino-acid epitope tag (termed g10) placed at the amino end of the protein. Immunization with a peptide representing the g10 epitope was described previously for the generation of antibodies reactive with various g10-tagged proteins (6, 33, 58). As shown in Fig. 4, transcripts containing in vitro-synthesized c-*fos*, GM-CSF, and c-*myc* 3′ UTR mRNAs were precipitable with anti-g10 serum with g10-tagged Hel-N1 (lanes 7 to 9).

TABLE 2. Relative binding of Hel-N1 and the U1snRNP-A proteins to RNAs shown in the binding experiments in Fig. 4[a]

RNA[b]	Hel-N1		U1snRNP-A	
	cpm	Ratio	cpm	Ratio
c-*myc* 3′ UTR	47,452	295	2,015	13
GM-CSF 3′ UTR	14,496	186	235	3
c-*fos* 3′ UTR	12,876	129	421	4
N-*myc* 3′ UTR	1,536	6	1,837	8
hY1 scRNA	374	4	299	3
U1 snRNA	1,470	11	21,390	154

[a] U1snRNP-A provided an internal control. cpm, total counts per minute bound in the RNA binding assay with the g10 epitope tag; ratio, the relative ratio of radioactivity bound per number of uridylate residues in each transcript.
[b] scRNA, small cytoplasmic RNA; snRNA, small nuclear RNA.

Quantitative comparison of radiolabeled transcripts containing the 3′ UTR of c-*myc*, c-*fos*, and GM-CSF demonstrated a strong binding to Hel-N1 compared with several control RNAs (Table 2). The specificity of Hel-N1 binding to these transcripts was substantiated with many control RNAs. For example, Fig. 4, lanes 10 to 12, demonstrates that U1snRNP-70K mRNA and hY1 antisense RNA, as well as the 3′ UTR of N-*myc*, respectively, did not bind to Hel-N1. Other control transcripts including precursor mRNA transcripts containing polypyrimidine-rich introns; U1 RNA, a transcript encoding neomycin resistance; various vector sequence transcripts; and noncoding regions of the dopamine 1 receptor mRNA failed to bind Hel-N1 (data not shown). In total, at least 15 different in vitro transcripts were examined as controls for RNA binding specificity, and all failed to bind to Hel-N1. Of particular interest was the finding that Hel-N1 bound c-*myc*, but not N-*myc*, 3′ UTRs. Although the c-*myc* and N-*myc* 3′ UTRs contain uridylate-rich regions, the c-*myc* 3′ UTR contains many characteristic short uridylate stretches, including three AUUUA pentamers, whereas the N-*myc* 3′ UTR lacks this pentamer. Furthermore, the N-*myc* 3′ UTR has not been identified among the oncoprotein and lymphokine mRNAs with instability regions. As a control for specificity of RNA binding under these conditions, the U1snRNP-A protein was able to bind efficiently to U1 RNA but not to other transcripts (Table 2). In the above experiments, c-*myc* mRNA showed the strongest binding to Hel-N1; thus, it was chosen as the model transcript for subsequent in vitro binding experiments although it may not be the in vivo Hel-N1 cognate RNA. As in our previous studies, RNA binding reactions were carried out in the presence of RNA competitors including tRNA and poly(A) (39, 40).

Sequences within the 3′ UTR of c-*myc* mRNA required for binding of Hel-N1. To delineate the mRNA sequence to which Hel-N1 binds, a series of transcripts progressively deleted from the 3′ end of the c-*myc* 3′ UTR were immunoprecipitated with g10-tagged Hel-N1 (Fig. 5). Binding to the full-length transcript of 432 nt and to 3′-truncated transcripts of 293, 219, and 181 nt was consistently strong (Fig. 5, lanes 5 to 7, and data not shown). However, removal of the 29-nt sequence 5′-UAACAGAUUUGUAUUUAAGAAUUGUUUUU-3′ from the 181-nt transcript decreased binding by Hel-N1 to an undetectable level (Fig. 5, lane 8). It is apparent that the loss of binding between positions 181 and 152 was due to recognition of all or part of the 29-nt sequence; however, we cannot rule out effects of secondary structure or other regions of the RNA that may be involved

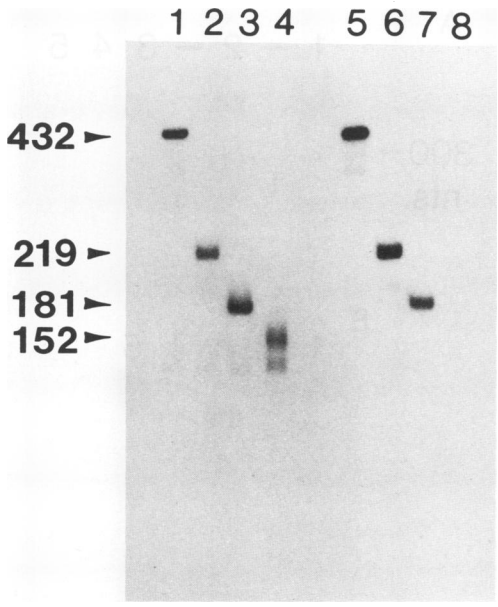

FIG. 5. Binding of Hel-N1 to various transcripts from the 3′ UTR of c-*myc* mRNA. The binding assay was identical to that used for Fig. 4. Supernatants (lanes 1 to 4) and bound ^{32}P-labeled RNA transcripts (lanes 5 to 8) from immunoprecipitation experiments used the following transcripts: *Bam*HI (432-nt, full-length transcript), *Ssp*I (219-nt transcript), *Dra*I (181-nt transcript), and *Mse*I (152-nt transcript) were as depicted in Fig. 2 and as described in Materials and Methods. Transcripts were analyzed on a urea–acrylamide gel.

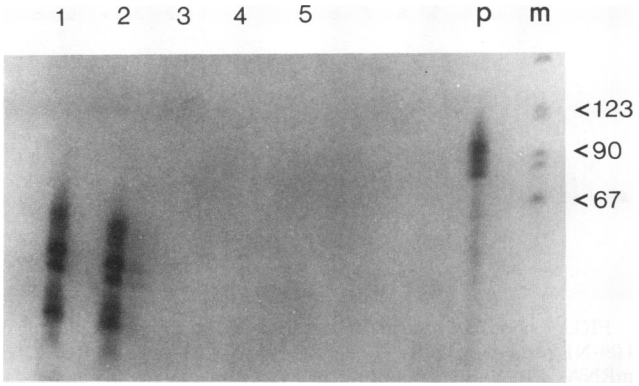

FIG. 6. Binding of Hel-N1 to c-*myc* 3′ UTR by coexpression in COS cells. Lane 1, transfection of COS cells with g10-tagged RRM3 and the 3′ UTR of c-*myc* followed by immunoprecipitation with g10 antibody and RNase protection; lane 2, transfection of COS cells with g10-tagged Hel-N1 and the 3′ UTR of c-*myc* followed by immunoprecipitation with g10-tagged antibody and RNase protection; lane 3, transfection of COS cells with a secretory alkaline phosphatase gene and the 3′ UTR of c-*myc* followed by immunoprecipitation with g10 antibody and RNase protection; lane 4, transfection of COS cells with g10-tagged Hel-N1 and the 3′ UTR of c-*myc* followed by immunoprecipitation with normal serum and RNase protection; lane 5, the RNA probe digested with RNase; lane p, undigested probe used for RNase protection; lane m, molecular weight markers.

in binding. The above sequence shows strong similarity in the underlined regions to RNA sequences selected from random pools as shown in Fig. 3 and Table 1.

One of the more common elements present in the 3′ UTR of the proto-oncogene and lymphokine RNAs is the pentamer AUUUA (8, 10, 12, 34, 51). This pentamer was present in the 29-nt sequence of the c-*myc* 3′ UTR found to be crucial for binding of Hel-N1. Shaw and Kamen (51) demonstrated that sequences from the 3′ UTR of GM-CSF containing six repeats of the AUUUA pentamer could, when placed in the noncoding region of the β-globin mRNA, reduce the half-life from 24 h to 30 min. The AUUUA pentamer was suggested to be an integral part of the instability consensus sequence (51) present in these 3′ UTRs, but a direct role for this sequence in mRNA stability has not been demonstrated unequivocally. Other regions of these mRNAs have also been implicated in instability (25, 30, 42, 52); however, studies of protein interactions with the 3′ UTR have focused on the conserved AUUUA pentamer as the major *cis* determinant of instability (34, 35, 60). As shown above, the hY1 transcript did not bind Hel-N1 despite the presence of an AUUUA pentamer. Although the 29-nt sequence delineated here contains a single AUUUA pentamer, the exact contact points between Hel-N1 and c-*myc* 3′ UTR are not known.

Demonstration of Hel-N1 binding to the 3′ UTR of c-*myc* mRNA in transfected COS cells. Having established that Hel-N1 could bind the 3′ UTR of oncogene and cytokine mRNAs in vitro, we obtained confirmatory evidence for this interaction with transient transfection. COS cells were transfected with DNA constructs encoding the 3′ UTR of c-*myc* mRNA together with control constructs encoding other mRNAs (Fig. 6). Constructs used in transient transfections included g10–Hel-N1, a secretory alkaline phosphatase gene, and a g10 construct encoding the carboxy-terminal 87 amino acids of Hel-N1 (Hel-N1/RRM3) (diagrammed in Fig. 1). After 48 h of incubation, cytoplasmic fractions were prepared and g10-containing proteins were immunoprecipitated with g10 rabbit antiserum. RNA in the immunoprecipitates was analyzed by RNase protection with a probe representing the first 42 nt of the 3′ UTR of c-*myc* mRNA. As shown in Fig. 6, lanes 1 and 2, both Hel-N1 and Hel-N1/RRM3 bound the c-*myc* transcript in cotransfected COS cells. Control experiments demonstrated that, in the absence of g10 antiserum (lane 4) or when a protein without a g10 epitope tag (lane 3) was used, the 3′ UTR of c-*myc* mRNA was not precipitable. The occurrence of multiple RNase-protected bands in lanes 1 and 2 was consistently observed with these probes and may be due to their low G+C content. These experiments demonstrate that Hel-N1 is capable of binding the 3′ UTR of c-*myc* mRNA in transfected COS cells. Further, these data suggest that Hel-N1/RRM3 alone was sufficient for binding the 3′ UTR of c-*myc*. As demonstrated below, this conclusion was corroborated further by additional binding experiments.

Hel-N1 forms multimeric complexes with c-*myc* and GM-CSF mRNA. As another confirmatory RNA binding method, we used mobility shift assays with radiolabeled transcripts of the 3′ UTR of c-*myc* and GM-CSF mRNAs. These transcripts were added to purified Hel-N1, and mobility shift analysis was performed as described previously (6, 33, 39, 40). Figures 7A and B show the results of addition of increasing amounts of partially purified Hel-N1 to c-*myc* or GM-CSF transcripts, respectively, followed by analysis on nondenaturing gels. Both transcripts were shifted to a series of slower-mobility bands as the amount of Hel-N1 was increased progressively from 0 to 2.5 μg of protein. The appearance of the multiple RNP bands detected in the mobility shift experiments suggests that Hel-N1 may form

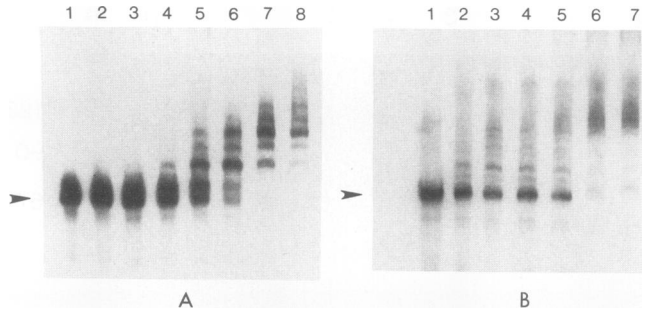

FIG. 7. Formation of multimers by mobility shift upon binding of Hel-N1 protein with the 3′ UTR of c-*myc* (A) and GM-CSF (B) mRNAs. Recombinant proteins were incubated in increasing amounts with ^{32}P-labeled transcripts of c-*myc* (219 nt) and GM-CSF (266 nt) 3′ UTR. After binding for 10 min, complexes were analyzed on 3.2% nondenaturing polyacrylamide gels. (A) Lanes: 1, in vitro transcript of 3′ UTR of c-*myc* mRNA; 2 to 8, addition of 0.05, 0.1, 0.2, 0.5, 1, 2, and 5 μl of purified Hel-N1 (0.5 μg/μl) preincubated with the c-*myc* mRNA transcript. (B) Lanes: 1, in vitro transcript of 3′ UTR of GM-CSF mRNA; 2 to 7, addition of 0.5, 1, 2, 3, 4, and 5 μl of purified Hel-N1 preincubated with the GM-CSF mRNA transcript.

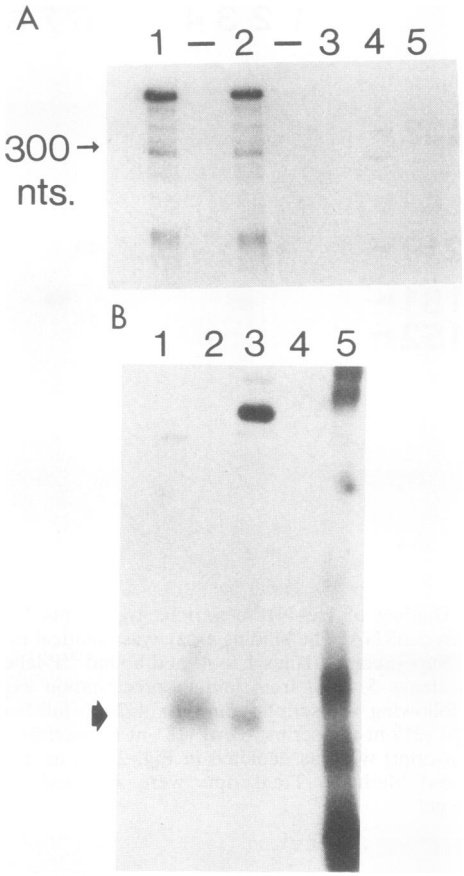

FIG. 8. (A) Immunoprecipitation of Hel-N1 bound to 3′ UTR of c-*myc* mRNA with PEM autoimmune serum and g10 serum. Lanes: 1, 3′ UTR of c-*myc* bound to Hel-N1 and immunoprecipitated with PEM autoantibody; 2, 3′ UTR of c-*myc* bound to Hel-N1 and immunoprecipitated with g10 antibody; 3, U1snRNP-70K mRNA bound to Hel-N1 and immunoprecipitated with PEM autoantibody; 4, hY1 antisense transcript bound to Hel-N1 and immunoprecipitated with PEM antibody; 5, 3′ UTR of N-*myc* mRNA bound to Hel-N1 and immunoprecipitated with PEM autoantibody. (B) Immunoprecipitation of Hel-N1 cross-linked to ^{32}P-labeled 3′ UTR of c-*myc* mRNA. Hel-N1 tagged with the g10 epitope was UV cross-linked and immunoprecipitated with anti-g10 serum or with PEM autoantiserum. Lanes: 1, immunoprecipitation with g10 antibody after UV cross-linking; 2, immunoprecipitation with PEM antibody after UV cross-linking; 3, UV cross-linking without immunoprecipitation; 4, RNase digestion before UV cross-linking; 5, no RNase and no antibody added after cross-linking. Samples were analyzed on SDS–10% polyacrylamide gels. The arrow denotes the position of Hel-N1′, which is approximately 28 kDa in size.

qualitatively different complexes with the GM-CSF 3′ UTR than with the c-*myc* 3′ UTR, although the exact composition of these complexes is not known. However, we have determined that the RNA present in each band is full length (data not shown). As with the Hel-N1 immunoprecipitation binding reactions, the mobility shift analyses were carried out in the presence of competitor tRNA, poly(A), and BSA. It should be noted that *E. coli* proteins were not responsible for these mobility shifts because the Hel-N1 protein was purified and in similar experiments using IPTG-induced *E. coli* extract alone multimers were not produced by mobility shift. Furthermore, our laboratory has used other RRM proteins in *E. coli* extracts, as well as purified RRM proteins, and none has been found to produce multimeric bands by mobility shift analysis (data not shown).

Hel-N1 and c-*myc* RNA form an autoantigenic RNP complex. Recent studies of paraneoplastic disorders associated with small cell lung carcinoma, including paraneoplastic cerebellar degeneration and PEM, have resulted in the identification of several autoantigens recognized by autoantibodies in the sera of patients with these disorders (15, 18, 54). One PEM-associated autoantigen, HuD, like Hel-N1 contains three RRMs, and the proteins share significant homology. As expected, recombinant Hel-N1 was also reactive with antiserum from PEM patients (data not shown).

Systemic autoantigens, classically exist as RNP particles which are reactive with autoantibodies (31). Thus, it was important to determine whether PEM autoantibodies can recognize Hel-N1 when bound to c-*myc* transcripts. When PEM autoantibodies were used in the RNA binding protocol in place of the g10 antiserum, c-*myc* transcripts were precipitable (Fig. 8A, lane 1), while control RNAs did not bind Hel-N1 in this assay (Fig. 8A, lanes 3 to 5). Similar results were obtained with GM-CSF transcripts, while four normal human serum samples lacked the ability to immunoprecipitate these complexes (data not shown).

We also determined whether a preformed complex containing UV-cross-linked Hel-N1 and the c-*myc* or the GM-CSF transcript could be recognized by PEM autoantiserum. Hel-N1 was incubated with ^{32}P-labeled c-*myc* or GM-CSF mRNAs and exposed to UV light to mediate covalent cross-linking between the RNA and associated proteins (35, 60). After UV cross-linking, excess RNA was digested with RNase A and the proteins were analyzed on SDS-acrylamide gels (Fig. 8B). The label transfer from c-*myc* RNA to Hel-N1 revealed two predominant bands of 85 and 28 kDa (Fig. 8B, lane 3). The higher-molecular-weight band was shown to result from *E. coli* proteins following IPTG induction, since UV cross-linking of control extracts lacking Hel-N1 also exhibited the larger band. In subsequent experiments using the partially purified recombinant Hel-N1, no bands other than Hel-N1 were observed. Using PEM autoantiserum, we found that the 28-kDa band, Hel-N1′, was precipitable (Fig. 8B, lane 2), while four normal human serum samples were

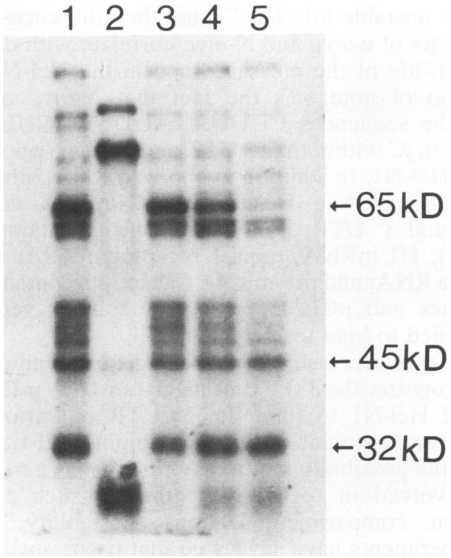

FIG. 9. Competition and binding assays by label transfer from ^{32}P-labeled 3′ UTR of c-*myc* mRNA to Hel-N1 and HeLa cell nuclear extract. Lane 1, label transfer to HeLa cell nuclear extract by UV cross-linking of ^{32}P-labeled c-*myc* mRNA; lane 2, label transfer to Hel-N1 by UV cross-linking of ^{32}P-labeled c-*myc* mRNA; lanes 3 to 5, addition of 1-, 2-, and 5-μl equivalents of Hel-N1 extract to the HeLa cell extract, respectively.

nonreactive (data not shown). These label transfer experiments consistently displayed Hel-N1 as a 28-kDa fragment (lane 2) which was reactive with PEM antibodies (data not shown). This band is 10 kDa smaller than the expected size of recombinant Hel-N1. This fragmentation was similar to results reported with two other RRM proteins which spontaneously fragment in vivo and in vitro (46, 55), but the functional implications of these observations are not clear. Interestingly, the g10 rabbit antiserum was not able to immunoprecipitate any of the UV-cross-linked proteins (Fig. 8B, lane 1), suggesting that Hel-N1′ lacked a 10-kDa fragment corresponding to the amino terminus of Hel-N1 and the g10 epitope tag.

The cause of the fragmentation of Hel-N1 is unknown, but it was consistently observed with the label transfer protocol. Nonetheless, our experiments demonstrate that PEM autoantibodies did not interfere with the ability of Hel-N1 to recognize and bind its RNA ligand as observed previously for other systemic autoantigenic RNA-binding proteins studied in our laboratory (6, 31, 33, 40). Furthermore, these data indicate that the RNA binding domain for the 3′ UTR of c-*myc* mRNA resides in a 28-kDa fragment containing at least the third RRM of Hel-N1 (Fig. 1).

UV cross-linking of 3′ UTR of c-*myc* to Hel-N1 in competition with proteins in HeLa nuclear extracts. Several studies have used label transfer to identify proteins that are capable of being UV-cross-linked to the 3′ UTR of c-*myc* (35, 60). To determine whether Hel-N1 can compete with cellular proteins for binding to c-*myc* mRNA, HeLa cell nuclear extracts and *E. coli* extracts containing recombinant Hel-N1 were incubated with ^{32}P-labeled c-*myc* 3′ UTR and exposed to UV light. After cross-linking, excess RNA was digested with RNase A and analyzed on an SDS-acrylamide gel (Fig. 9, lanes 1 and 2). When increasing amounts of Hel-N1 were added to the nuclear extract prior to UV cross-linking, a band of about 65 kDa was reduced by the competition with Hel-N1; however, its identity is unknown (Fig. 9, lanes 3 to 5). A 32-kDa protein band identified previously as being capable of cross-linking to c-*myc* 3′ UTR (60) was not diminished significantly (Fig. 9, lanes 3 to 5). It is possible that the 65-kDa protein may recognize similar structures and sequences in the 3′ UTR which are in close proximity to those bound by Hel-N1. Thus, it will be interesting to examine the sequence and RNA binding properties of the 65-kDa protein and to determine whether it is involved in processing and/or instability of HeLa cell mRNAs.

Defining the c-*myc* mRNA binding domain of Hel-N1. In order to understand the functional significance of RNA-protein interactions, it is important to define the binding characteristics of the respective ligands. Query et al. (39) defined the U1 RNA binding domain of the U1-70K protein with an in vitro binding assay and transcripts of U1 small nuclear RNA. However, many RNA-binding proteins possess RRMs for which the RNA targets are not known (reviewed in reference 27). In some cases, proteins which possess more than one RRM, like Hel-N1, may have RNA targets identified for only one of the RRMs. For example, the U1A and U2B″ proteins each possess two RRMs, but the amino-terminal RRM of each is sufficient for binding U1 and U2 RNAs, respectively (6, 33, 49). The carboxy-terminal RRMs of U1A and U2B″ do not have known RNA binding targets, and thus the amino acid residues which constitute these RNA binding domains have not been assigned. Similarly, poly(A)-binding protein consists of four RRMs, only a subset of which have been shown to bind to poly(A); the function of the other RRM(s) is presently unknown (11, 27, 37).

As suggested from the data of Fig. 6, RRM3 of Hel-N1 alone may possess 3′ UTR binding activity. To determine whether RRM3 of Hel-N1 can function as an independent RNA binding domain for c-*myc*, 3′ UTR deletion mutants (Fig. 1) that expressed either RRM1 (termed Hel-N1/RRM1), RRM 1 and most of RRM2 (termed Hel-N1/RRM1,2′), or an 87-amino-acid protein containing only RRM3 (termed Hel-N1/RRM3) were constructed. Of the three deletion constructs, only Hel-N1/RRM3 lacked the amino terminus of the native Hel-N1. Figure 10 demonstrates that Hel-N1/RRM3 alone (lane 3) was sufficient for binding the 3′ UTR of c-*myc* mRNA with the immunoprecipitation RNA binding assay. There was no detectable binding to Hel-N1/RRM1 or to Hel-N1/RRM1,2′ fragments (Fig. 10, lanes 1 and 2) even when varying amounts of protein were used. We conclude that the 87-amino-acid fragment containing RRM3 of Hel-N1 constitutes an RNA binding domain for the 3′ UTR of c-*myc* mRNA.

DISCUSSION

Determining an RNA ligand for putative RNA-binding proteins is a particularly difficult problem. The most common approach involves direct in vitro binding of radiolabeled cellular RNA and sequencing or probing for bound ligands. Unfortunately, only highly abundant RNAs or highly stable RNAs are usually detectable by these methods. More recently, selection from random or degenerate pools of nucleic acids has proved useful for identifying binding sequences for DNA- and RNA-binding proteins (5, 56, 59). In this study, we used an in vitro selection protocol from random RNA to delineate preferred binding sequences for Hel-N1. The objective of this approach is to gain insights into potential biological ligands. Thus, it is not always necessary that a

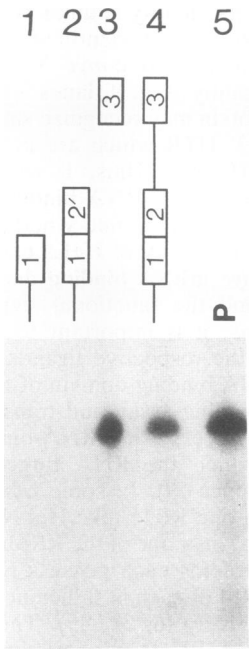

FIG. 10. RRM3 of Hel-N1 constitutes an RNA binding domain for 3′ UTR of c-*myc* mRNA. Deletion mutants of Hel-N1 containing RRM1 (lane 1) RRM1,2′ (lane 2), RRM3 (lane 3), and full-length Hel-N1 (lane 4) were expressed in *E. coli*. Each expressed protein construct was tested for its ability to bind c-*myc* 3′ UTR mRNA by immunoprecipitation using the g10 serum as described in the legend to Fig. 4 and Materials and Methods. Lane 5 shows the c-*myc* 3′ UTR transcript used in the binding reactions; P represents probe alone.

single unique consensus sequence be derived by this in vitro method.

Derivation of a sequence of character involving short stretches of uridylates which were selected by Hel-N1 proved sufficient to lead us to the growth factor 3′ UTRs. Regardless of whether the particular mRNAs shown in Table 1 are native ligands for Hel-N1, they represent valuable and interesting biological targets with which to study its binding. Thus, we were able to demonstrate direct RNA binding of Hel-N1 to the 3′ UTRs of c-*myc*, GM-CSF, and c-*fos* mRNAs. Several confirmatory methods including immunoprecipitation, label transfer, and mobility shift assays consistently demonstrated the specificity of RNA binding in vitro. In addition, we demonstrated that an 87-amino-acid sequence comprising the third RRM of Hel-N1 is, by itself, capable of binding the 3′ UTR of c-*myc*. These findings were confirmed further by cotransfecting Hel-N1 and the 3′ UTR of c-*myc* transiently into COS cells.

We employed several controls to validate the specificity of Hel-N1 binding to the 3′ UTRs of these mRNAs. Perhaps the most interesting controls were the coding and noncoding regions of N-*myc* which were unable to bind Hel-N1. This result is curious given that c-*myc* and N-*myc* have highly similar amino acid sequences and that both proteins have been implicated in neuronal growth and development (2, 9, 20). However, significant differences reside in the 3′ UTRs of c-*myc* and N-*myc* mRNAs (16). The N-*myc* 3′ UTR, although uridylate rich, lacks sequences characteristic of those selected and shown in Fig. 3 and noted by others to reside among the instability sequences (51). Therefore, N-*myc* has not been grouped with c-*myc*, GM-CSF, c-*fos*, and other unstable mRNAs. Thus, the differences between the 3′ UTRs of c-*myc* and N-*myc* correlate with differences in the half-life of the messages and in the Hel-N1 binding data. Also of note was the fact that N-*myc* transcripts contain the sequences CUUUA, AUUUG, CUUUC, and $G(U)_5G(U)_{10}C$ within the 5′ UTR and coding regions but do not bind Hel-N1. In addition to N-*myc* mRNA, other control transcripts including U1snRNP-70K mRNA coding sequences and 3′ UTR; hY1 RNA (which contains a single AUUUA); U1 mRNA; dopa-1 receptor mRNA; neomycin resistance RNA; and pre-mRNA transcripts containing polypyrimidines and pGEM3, pSP64, and other vector transcripts failed to bind to Hel-N1.

Hel-N1 may represent a *trans*-acting RNA-binding protein which recognizes the 3′ UTR of highly unstable mRNAs. The ability of Hel-N1 to bind the 3′ UTR of various proto-oncogene and cytokine mRNAs containing AU-rich regions suggests the possibility that it may function as a *trans*-acting factor involved in regulatory pathways such as mRNA translation, compartmentalization, or stability. Although other experiments have suggested that tissue-specific *trans*-acting factors can affect the half-life of mRNAs containing AU-rich 3′ UTRs (50), none of these factors has been elucidated. Hel-N1 is a potential candidate for such a factor on the basis of its in vitro binding to growth factor mRNAs. However, no direct role for Hel-N1 in regulating these processes has yet been demonstrated.

Levels of c-*myc* and other growth factors are known to change during development as withdrawal from the cell cycle appears to be a prerequisite for commitment to terminal differentiation (13, 14, 53). It is possible that Hel-N1 and related proteins participate in neuronal development by affecting growth factor mRNAs. Furthermore, Hel-N1 may represent a group of tissue-specific proteins that participate in regulating growth factors involved in the differentiation of various cell types (14, 20, 22). Such a model is compatible with the genetic phenotype of *elav* which has been shown to function in differentiation and migration of neuroblasts into adult neurons (23, 44).

It is interesting to note that K3(*rbp9*) contains a distinct CT repeat transcription promoter element that also exists in the *myc* homolog of *D. melanogaster*, *achaete-scute* (28). Both K3(*rbp9*) and *achaete-scute*, as well as *elav*, are implicated in neurogenesis in *D. melanogaster*. We have noted that the 3′ UTRs of *achaete-scute t4* and *t5* mRNAs (61) contain the RNA sequences selected to bind Hel-N1 and common to the growth factor mRNAs shown in Fig. 3. Thus, it will be important to determine whether direct interactions can occur between *achaete-scute* mRNAs and *elav* or K3(*rbp9*) proteins.

The *elav*-like proteins, including Hel-N1, HuD, and K3(*rbp9*) contain highly similar RRMs, which makes it likely that they bind to similar RNA target sequences. As a group, the *elav*-like RRMs appear related to the *D. melanogaster* splicing protein, *Sex lethal* (29), and to some heterogeneous nuclear RNP proteins, especially in the RNP1 octamer regions (29a). Thus, it is possible that *elav*, K3(*rbp9*), HuD, and Hel-N1 are members of a subgroup of RRM proteins which bind to both precursor and mature mRNAs. For example, it is possible that Hel-N1 can bind to pre-mRNA sequences such as the polypyrimidine tracts of yet-unknown pre-mRNAs, while functioning also at the 3′ UTR on the mature mRNA. This possibility is consistent with the proposal of Pinol-Roma and Dreyfuss that certain heterogeneous nuclear RNP proteins appear to cycle between the nucleus and the cytoplasm (38). However, complete analysis

of the in vivo localization and cellular RNA targets of Hel-N1 and related proteins will be necessary to implicate them as regulatory RRM proteins with such dual functions.

Implications for autoimmunity and cancer. The observation that Hel-N1, like HuD, is reactive with an autoantibody present in the serum of patients with PEM (54) puts it in the category of other human autoantigens that are members of the RRM superfamily (26, 41, 47). Furthermore, the ability of Hel-N1 to bind to growth factor mRNAs as an RNP complex is intriguing since PEM patients are a subset of those afflicted with small cell lung cancer, a disease in which levels of c-*myc* are elevated (7, 24, 32). Although we have not precisely mapped the epitopes recognized by PEM patients, we have observed that the PEM serum does not react with RRM3. This is consistent with the finding that autoantibody recognition of Hel-N1 did not interfere with binding to c-*myc* RNA (Fig. 8A). While these findings suggest a potential link between an autoimmune response and oncogenesis, the precise origins of autoantibodies to Hel-N1 remain as elusive as with the other systemic autoantigens (47).

The c-*myc* oncogene is known to be activated or amplified in a number of naturally occurring neuronal tumors, including small cell lung cancer (7, 24, 32), medulloblastomas (9), and neuroendocrine tumors (2). Although no direct link between occurrence of these tumors and expression of Hel-N1 has been demonstrated, studies of the interactions of Hel-N1 and other *elav*-like proteins with growth factor mRNAs should help provide a better understanding of their role in autoimmunity and cancer.

ACKNOWLEDGMENTS

We thank Joelle Romac, Ameeta Kelekar, and Dan Kenan for advice throughout these studies.

This work was supported by research grants from the National Institutes of Health to J.D.K. L.G.A. was supported by an NIH Tumor Immunology Postdoctoral Training Grant, P.H.K. was supported by an NIH Neurobehavioral Postdoctoral Training Grant, and T.D.L. was supported by the Four Schools Physician-Scientist Program.

REFERENCES

1. **Adam, S. A., T. Nakagawa, M. S. Swanson, T. K. Woodruff, and G. Dreyfuss.** 1986. mRNA polyadenylate-binding protein: gene isolation and sequencing and identification of a ribonucleoprotein consensus sequence. Mol. Cell. Biol. **6**:2932–2943.
2. **Alitalo, K., M. Schwab, C. C. Lin, H. E. Varmus, and J. M. Bishop.** 1983. Homogeneously staining chromosomal regions contain amplified copies of an abundantly expressed cellular oncogene (c-myc) in malignant neuroendocrine cells from a human colon carcinoma. Proc. Natl. Acad. Sci. USA **80**:1707–1711.
3. **Ayane, M., U. Preuss, G. Kohler, and P. T. Nielsen.** 1991. A differentially expressed murine RNA encoding a protein with similarities to two types of nucleic acid binding motifs. Nucleic Acids Res. **19**:1273–1278.
4. **Bandzuilis, R. J., S. Swanson, T. K. Woodruff, and G. Dreyfuss.** 1986. RNA binding proteins as developmental regulators. Genes Dev. **3**:431–437.
5. **Bartel, D. P., M. Z. Zapp, M. R. Green, and J. W. Szostak.** 1991. HIV-1 Rev regulation involves recognition of non-Watson-Crick base pairs in viral RNA. Cell **67**:529–536.
6. **Bentley, R. C., and J. D. Keene.** 1991. Recognition of U1 and U2 small nuclear RNAs can be altered by a 5-amino-acid segment in the U2 small nuclear ribonucleoprotein particle (snRNP) B″ protein and through interactions with U2 snRNP-A′ protein. Mol. Cell. Biol. **11**:1829–1839.
7. **Bepler, G., H. Bading, B. Heiman, P. Kiefer, B. Havemann, and K. Moelling.** 1989. Expression of p64 c-myc and neuroendocrine properties define 3 subclasses of small cell lung cancer. Oncogene **4**:45–50.
8. **Bernstein, P. L., J. D. Herrick, R. D. Prokipcak, and J. Ross.** 1992. Control of c-myc mRNA half-life in vitro by a protein capable of binding to a coding region stability determinant. Genes Dev. **6**:642–654.
9. **Bigner, S. H., H. S. Friedman, B. Vogelstein, W. J. Oakes, and D. D. Bigner.** 1990. Amplification of the c-myc gene in human medulloblastoma cell lines and xenografts. Cancer Res. **50**: 2347–2350.
10. **Brewer, G., and J. Ross.** 1988. Poly(A) shortening and degradation of the 3′ A+U-rich sequences of human c-*myc* mRNA in a cell-free system. Mol. Cell. Biol. **8**:1697–1703.
11. **Burd, C. G., E. L. Matunis, and G. Dreyfuss.** 1991. The multiple RNA-binding domains of the mRNA poly(A)-binding protein have different RNA-binding activities. Mol. Cell. Biol. **11**:3419–3424.
12. **Caput, D., B. Beutler, K. Hartog, R. Thayer, S. Brown-Schimmer, and A. Cerami.** 1986. Identification of a common nucleotide sequence in the 3′ untranslated region of mRNA molecules specifying inflammatory mediators. Proc. Natl. Acad. Sci. USA **83**:1670–1674.
13. **Chamberlain, J. S., J. B. Jaynes, and S. D. Hauschka.** 1985. Regulation of creatine kinase induction in differentiating mouse myoblasts. Mol. Cell. Biol. **5**:484–492.
14. **Cole, M. D.** 1986. The myc oncogene: its role in transformation and differentiation. Annu. Rev. Genet. **20**:361–384.
15. **Dalmau, J., H. M. Furneaux, R. J. Gralla, M. G. Kris, and J. B. Posner.** 1990. Detection of the anti-Hu antibody in the serum of patients with small cell lung cancer—a quantitative Western blot analysis. Ann. Neurol. **27**:544–552.
16. **Depinho, R. A., E. Legouy, L. B. Feldman, N. E. Kohl, G. C. Yancopoulos, and F. W. Alt.** 1986. Structure and expression of the murine N-myc gene. Proc. Natl. Acad. Sci. USA **83**:1827–1831.
17. **Dignam, J. D., R. M. Lebovitz, and R. G. Roeder.** 1983. Accurate transcription initiation by RNase polymerase II in a soluble extract from isolated mammalian nuclei. Nucleic Acids. Res. **11**:1475–1489.
18. **Dropcho, E. J., Y. T. Chen, J. B. Posner, and L. J. Old.** 1987. Cloning of a brain protein identified by autoantibodies from a patient with paraneoplastic cerebellar degeneration. Proc. Natl. Acad. Sci. USA **84**:4552–4556.
19. **Ernfors, A. D., and J. W. Szostak.** 1990. In vitro selection of RNA molecules that bind specific ligands. Nature (London) **346**:818–822.
20. **Hammerling, U., C. Bjelfman, and S. Pahlman.** 1987. Different regulation of N- and c-myc expression during phorbolester-induced maturation of SH-SY5Y neuroblastoma cells. Oncogene **2**:73–77.
21. **Hoffman, D. W., C. C. Query, B. L. Golden, S. W. White, and J. D. Keene.** 1991. The RNA binding domain of an snRNP protein is structurally related to ribosomal proteins. Proc. Natl. Acad. Sci. USA **88**:2495–2499.
22. **Javala, A. M., J. E. Heikkila, and K. E. O. Akerman.** 1988. Decline in c-myc mRNA expression but not the induction of c-fos mRNA expression is associated with differentiation of SH-SY5Y human neuroblastoma cells. Exp. Cell Res. **179**:10–17.
23. **Jiminez, F., and K. E. O. Campos-Ortega.** 1979. A region of the *Drosophila* genome necessary for CNS development. Nature (London) **282**:310–312.
24. **Johnson, B. E., R. W. Makuch, A. B. Simmons, A. F. Gazdan, D. Burch, and A. W. Cashell.** 1988. Myc family DNA amplification in small cell lung cancer patients' tumors and corresponding cell lines. Cancer Res. **48**:5163–5166.
25. **Jones, T. R., and M. D. Cole.** 1987. Rapid cytoplasmic turnover of c-*myc* mRNA: requirement of the 3′ untranslated sequences. Mol. Cell. Biol. **7**:4513–4521.
26. **Keene, J. D., and C. C. Query.** 1991. Nuclear RNA binding proteins. Prog. Nucleic Acid Res. Mol. Biol. **41**:179–202.
27. **Kenan, D. J., C. C. Query, and J. D. Keene.** 1991. RNA recognition: towards identifying determinants of specificity.

Trends Biochem. Sci. **16:**214–220.
28. **Kim, Y.-J., and B. S. Baker.** 1993. The Drosophila gene rbp9 encodes a protein that is a member of a conserved group of putative RNA binding proteins that are nervous system-specific in both flies and humans. J. Neurosci. **13:**1045–1056.
29. **Kim, Y.-J., and B. S. Baker.** 1993. Isolation of RRM-type RNA-binding protein genes and the analysis of their relatedness by using a numerical approach. Mol. Cell. Biol. **13:**174–183.
29a. **King, P. H., T. D. Levine, R. T. Fremeau, and J. D. Keene.** Unpublished data.
30. **Laird-Offringa, I. A., P. Elfferich, and A. J. van der Eb.** 1991. Rapid c-myc mRNA degradation does not require (A+U)-rich sequences or complete translation of the mRNA. Nucleic Acids Res. **19:**2387–2394.
31. **Lerner, M. R., and J. A. Steitz.** 1979. Antibodies to small nuclear RNAs complexed with proteins are produced by patients with systemic lupus erythematosus. Proc. Natl. Acad. Sci. USA **76:**5495–5499.
32. **Little, C. D., M. M. Lau, D. N. Carney, A. F. Gazdar, and J. D. Minna.** 1983. Amplification and expression of the c-myc oncogene in human lung cancer cell lines. Nature (London) **306:**194–196.
33. **Lutz-Freyermuth, C., C. C. Query, and J. D. Keene.** 1990. Quantitative demonstration that only one of two potential RNA-binding domains of the U1snRNP-A protein is required for specific binding to U1 RNA. Proc. Natl. Acad. Sci. USA **87:**6393–6397.
34. **Malter, J. S.** 1989. Identification of an AUUUA-specific messenger RNA binding protein. Science **246:**664–666.
35. **Myer, V. E., S. I. Lee, and J. A. Steitz.** 1992. Herpes virus saimiri encoded U RNAs bind a 32 KD protein implicated in mRNA degradation. Proc. Natl. Acad. Sci. USA **89:**1296–1300.
36. **Nagai, K., C. Oubridge, T. H. Jessen, J. Li, and P. R. Evans.** 1990. Crystal structure of the RNA-binding domain of the U1 small nuclear ribonucleoprotein A. Nature (London) **348:**515–520.
37. **Nietfield, W., H. Mentzel, and T. Pieler.** 1990. The *Xenopus leavis* poly (A) binding protein is composed of multiple functionally independent RNA binding domains. EMBO J. **9:**3699–3705.
38. **Pinol-Roma, S., and G. Dreyfuss.** 1992. Shuttling of pre-mRNA binding proteins between nucleus and cytoplasm. Nature (London) **355:**730–732.
39. **Query, C. C., R. C. Bentley, and J. D. Keene.** 1989. A common RNA recognition motif identified within a defined U1 RNA binding domain of the 70K U1 snRNP protein. Cell **57:**89–101.
40. **Query, C. C., R. C. Bentley, and J. D. Keene.** 1989. A specific 31-nucleotide domain of U1 RNA directly interacts with the 70K small nuclear ribonucleoprotein component. Mol. Cell. Biol. **9:**4872–4881.
41. **Query, C. C., and J. D. Keene.** 1987. A human autoimmune protein associated with U1 RNA contains a region of homology that is cross-reactive with retroviral p30gag antigen. Cell **51:**211–220.
42. **Rabbitts, P. H., A. Forster, M. A. Stinson, and T. H. Rabbitts.** 1985. Truncation of exon 1 from the c-myc gene results in prolonged c-myc RNA stability. EMBO J. **4:**3727–3733.
43. **Robinow, S., A. R. Campos, K.-M. Yao, and K. White.** 1988. The *elav* gene product of *Drosophila*, required in neurons, has the RNP consensus motifs. Science **242:**1570–1572.
44. **Robinow, S., and K. White.** 1988. The locus *elav* of *Drosophila melanogaster* is expressed in neurons at all developmental stages. Dev. Biol. **126:**294–303.
45. **Rosenberg, A. H., B. N. Lade, D. S. Chui, J. J. Dunn, and F. W. Studier.** 1987. Vectors used for selective expression of cloned DNAs by T7 polymerase. Gene **56:**125–135.
46. **Sachs, A. B., M. W. Bond, and R. D. Kornberg.** 1986. A single gene from yeast for both nuclear and cytoplasmic polyadenylate binding protein domain structure and expression. Cell **45:**827–835.
47. **Saitta, M., and J. D. Keene.** 1993. Soluble ribonucleoprotein antigens, p. 179–210. *In* M. H. V. Van Regenmortel (ed.), The antigens. CRC Press, Inc., Boca Raton, Fla.
48. **Sambrook, J., E. F. Fritsch, and T. Maniatis.** 1989. Molecular cloning: a laboratory manual, 2nd ed. Cold Spring Harbor Laboratory Press, Cold Spring Harbor, N.Y.
49. **Scherly, D., N. A. Dathan, W. Boelens, W. J. van Venrooij, and I. W. Mattaj.** 1990. The U2B″ RNA motif as a site of protein-protein interaction. EMBO J. **9:**3675–3681.
50. **Schuler, G. D., and M. D. Cole.** 1988. GM-CSF and oncogene mRNA stabilities are independently regulated in *trans* in a mouse monocytic tumor. Cell **55:**1115–1122.
51. **Shaw, G., and R. Kamen.** 1986. A conserved AU sequence from the 3′ untranslated region of GM-CSF mRNA mediates selective mRNA degradation. Cell **46:**659–667.
52. **Shyu, A. B., M. E. Greenberg, and J. G. Belasco.** 1989. The c-fos transcript is targeted for rapid decay by two distinct mRNA degradation pathways. Genes Dev. **3:**60–72.
53. **Sorrentino, V., R. Pepperkok, R. L. Davis, W. Ansorge, and L. Phillipson.** 1990. Cell proliferation inhibited by MYOD1 independently of myogenic differentiation. Nature (London) **345:**813–815.
54. **Szabo, A., J. Dalmau, G. Manley, M. Rosenfeld, E. Wong, J. Henson, J. B. Posner, and H. M. Furneaux.** 1991. HuD, a paraneoplastic encephalomyelitis antigen, contains RNA-binding domains and is homologous to elav and sex-lethal. Cell **67:**325–333.
55. **Tian, Q., H. M. Streuli, M. Saito, S. F. Schlossman, and P. Anderson.** 1991. A polyadenylate binding protein localized to the granules of cytolytic lymphocytes induces DNA fragmentation. Cell **67:**629–639.
56. **Tsai, D. E., D. S. Harper, and J. D. Keene.** 1991. U1-snRNP-A protein selects a ten nucleotide consensus sequence from a degenerate RNA pool presented in various structural contexts. Nucleic Acids Res. **19:**4931–4936.
57. **Tsai, D. E., and J. D. Keene.** 1993. In vitro selection of RNA epitopes using autoimmune patient serum. J. Immunol. **150:**1137–1145.
58. **Tsai, D. E., D. J. Kenan, and J. D. Keene.** 1992. In vitro selection of an RNA epitope immunologically cross reactive with a peptide. Proc. Natl. Acad. Sci. USA **89:**8864–8869.
59. **Tuerk, C., and L. Gold.** 1990. Systematic evolution of ligands by exponential enrichment: RNA ligands to bacteriophage T4 DNA polymerase. Science **249:**505–509.
60. **Vakalopoulou, E., J. Schaak, and T. Shenk.** 1991. A 32-kilodalton protein binds to AU-rich domains in the 3′ untranslated regions of rapidly degraded mRNAs. Mol. Cell. Biol. **11:**3355–3364.
61. **Villares, R., and C. V. Cabrera.** 1987. The achaete-scute gene complex of D. melanogaster: conserved domains in a subset of genes required for neurogenesis and their homology to myc. Cell **50:**415–424.
62. **von Besser, H., P. Schanbel, C. Wieland, E. Fritz, R. Sianewsky, and H. Saumweber.** 1990. The puff specific Drosophila protein Bj6, encoded by the gene no-on transient A, shows homology to RNA binding proteins. Chromosoma **100:**37–47.
63. **Wilusz, J., D. I. Feng, and T. Shenk.** 1988. The C proteins of heterogeneous nuclear ribonucleoprotein complexes interact with RNA sequences downstream of polyadenylation cleavage sites. Mol. Cell. Biol. **8:**4177–4183.